On the Jump Dynamics and Jump Risk Premiums

Gang Li[*]

January, 2017

On the Jump Dynamics and Jump Risk Premiums

Abstract

Extreme events, such as market crashes, are important to market participants because they have significant impacts on the welfare of investors. Such events are modeled as jumps in the stochastic processes of asset prices. This paper proposes a semi-parametric approach to examining jump dynamics, and finds that among popular specifications proposed in the literature, the model with an autoregressive jump intensity and a mixture of the exponential and generalized extreme value jump size distribution best characterizes the jump dynamics. The paper also shows that jump risks carry significant premiums, and the jump risk premiums are high when the growths of consumption and production in the economy are low and when the credit risk and volatility are high.

1. Introduction

In the theoretical and empirical studies of asset pricing, understanding the asset price dynamics and the risk premiums associated with various sources of the dynamics is a central topic. Jumps, which are used to model extreme events, such as market crashes, are essential components in the asset price dynamics. Because jumps are rare and not directly observable, their properties are difficult to analyze. While approaches have been proposed to characterize the jump dynamics in a growing literature, there is no consensus on how jumps should be modeled. In this paper, we examine various specifications of jump dynamics proposed in the literature, and shed light on how to model the jump dynamics.

Two elements are essential in modeling the jump dynamics, the jump arrival intensity process, i.e., the timing of jumps, and the distribution of jump sizes. Early studies on the asset price dynamics and option pricing assume that the jump intensity is constant, for example, Merton (1976). More recent studies assume that the conditional jump intensity is an affine and increasing function of the diffusive variance of the asset returns, for example, Bates (2000), Pan (2002) and Eraker (2004), among others. This is based on the idea that jumps tend to occur when the diffusive variance is high. There is another line of research which models the conditional jump intensity as a function of realized past jumps and past jump intensity, based on the observations that large price changes occur in clusters. This autoregressive type of models include Chan and Maheu (2002), Maheu and McCurdy (2004), Yu (2004), Santa-Clara and Yan (2010), Christoffersen, Jacobs and Ornthanalai (2012), Maheu, McCurdy and Zhao (2013), Aït-Sahalia, Cacho-Diaz and Laeven (2015), and Fulop, Li and Yu (2015). There is no consensus in the literature on which types of models characterize the jump dynamics better and whether they significantly improve upon the models with the constant jump intensity. Pan (2002) and Eraker (2004) find that allowing the dependence of conditional jump intensity on diffusive variance improves the performance of pricing the S&P 500 index options upon

the constant jump intensity model, however, Andersen, Benzoni and Lund (2002) find that when fitting the models to the S&P 500 index returns, the coefficient on the diffusive variance in the affine specification of jump intensity is not significant. Li and Zhang (2016) examine the issue using a nonparametric approach and find no relationship between the conditional jump intensity and diffusive variance for many indexes and stocks. Bates (2000) finds that there is no relation between the conditional jump intensity and diffusive variance under the physical probability, but there is a positive relation under the risk-neutral probability. In addition, the jump size is typically assumed to be independent of the conditional jump intensity, and to follow a distribution with fixed parameters. The normal and double exponential distributions are the most commonly used.[1] In this paper, we examine which combinations of the jump intensity and jump size distribution specifications fit the data better.

The properties of jumps are difficult to analyze also because jump dynamics can be affected by the restrictions imposed on other components in the asset price dynamics. The specifications of the stochastic volatility process are particulary important because both volatility and jumps are measures of the magnitude of possible future price changes. Recent studies have shown that many standard asset pricing models are mis-specified. Jones (2003) finds that the square-root stochastic volatility model is incapable of generating realistic return behavior and the data are better represented by a stochastic volatility model in the constant-elasticity-of-variance class or a model with a time-varying leverage effect. Christoffersen, Jacobs and Mimouni (2010) find that a stochastic volatility model with a linear diffusion term is more consistent with the data on the underlying asset and options than a stochastic volatility model with a square-root diffusion term is. Li and Zhang (2013) show that the affine drift of the diffusive volatility model is mis-specified

---

[1]In Andersen, Benzoni and Lund (2002), Bates (2000), Chan and Maheu (2002), Christoffersen, Jacobs and Ornthanalai (2012), Eraker (2004), Maheu and McCurdy (2004), Maheu, McCurdy and Zhao (2013), Pan (2002) and Santa-Clara and Yan (2010), the jump size is assumed to follow the normal distribution, whereas in Aït-Sahalia, Cacho-Diaz and Laeven (2015) and Kou (2002), the jump size is assumed to follow the double exponential distribution.

because the mean reversion is particularly strong at the high end of volatility. A robust analysis of the jump dynamics requires mitigating the impacts of the mis-specification of the stochastic volatility process.

This paper proposes an approach to estimating the jump dynamics and the associated risk premiums. Different from the approaches in the existing literature, we adopt a two-step semi-parametric approach. In the first step, the diffusive volatility is estimated by a jump-robust nonparametric approach. Since the analysis of the jump dynamics is sensitive to the model specifications of the stochastic volatility process, the nonparametric approach allows more robust inferences on the jump dynamics. In the second step, given the estimated diffusive volatility, the specifications of the conditional jump intensity and jump size distribution are estimated and tested. Our approach is applied to the daily returns of the S&P 500 index from 1950 to 2014. We find that the autoregressive jump intensity fits the data better than the constant and the affine jump intensities do. The double exponential distribution works better than the normal distribution for modeling the jump sizes. A mixture of the exponential distribution and the generalized extreme value distribution further improves the fit. The improvement is due to the ability of the generalized extreme value distribution to capture the fat tail of negative jumps. The jump risk premiums are inferred from the differences between the expected value of a jump measure under the risk-neutral probability and its physical counterpart. A high value of the jump measure indicates a high jump arrival intensity or jump size with a large magnitude or both. The jump measure under the risk-neutral probability is estimated from the S&P 500 index option prices in a model-free manner, and the one under the physical probability is estimated from the best specification of the jump arrival intensity and jump size distribution in the previous analysis. We find that the jump risk premiums are positive and large on average, and are strongly related to the macroeconomic conditions. In particular, the jump risk premiums are high when the growths of consumption and production in the economy are low and when the credit risk and volatility are high.

3

The rest of the paper is organized as follows. Section 2 discusses the specifications of the jump intensity process and the jump size distribution, and the estimation methodology. Section 3 presents the estimation results. Section 4 introduces the jump measure, defines the jump risk premiums, and reports the empirical results on the jump risk premiums. Section 5 concludes the paper.

2.   Empirical Methodology

Suppose that under the physical probability, the log price of an asset, S_u, is governed by the following process,

$$dS_u = \mu_u du + \sqrt{V_u} dW_u + Z_u dJ_u, \tag{1}$$

where μ_u is the instantaneous drift, V_u is the instantaneous diffusive variance, W_u is the Brownian motion, J_u is a Poisson process with time-varying and finite intensity λ_u, and Z_u is the jump size, independent of W_u and J_u. The focus of the analysis in this paper is how to model Z_u and λ_u, and the premiums associate with them.

Our estimation approach can be summarized as follows. First, we estimate V_u using a nonparametric approach without assuming the dynamics of V_u. Since the restrictions imposed on the dynamics of V_u inevitably affect the dynamics of Z_u and λ_u, the nonparametric approach to estimating V_u allows robust inferences on the dynamics of Z_u and λ_u. In the second step, given the estimated diffusive variance, we estimate some popular specifications of the jump arrival intensity and jump size distribution, and compare these specifications.

2.1.   Specifications of Conditional Jump Intensity and Jump Size Distribution

We introduce the specifications of conditional jump intensity and jump size distribution considered in this paper. The conditional jump intensity characterizes the timing of jump

4

arrivals. We consider three popular cases. The first is the constant jump intensity, i.e., $\lambda_u = \lambda$ for all u, where $\lambda \geq 0$. This is the simplest case, introduced by Merton (1976) in the option pricing literature, to account for non-normality of the return distribution. The second is the affine specification,

$$\lambda_u = \lambda_0 + \lambda_1 V_u, \tag{2}$$

where $\lambda_0 \geq 0$ and $\lambda_1 \geq 0$. The affine specification allows the time-varying jump intensity, and is build upon the intuition that when the diffusive volatility is higher, jumps are more likely to occur. The affine specification is popular because together with the square-root process of V_u as in Heston (1993), it admits a closed-form solution of the option price, for example, in Duffie, Pan, and Singleton (2000). The third is the autoregressive jump intensity. We take the self-exciting jump process in the continuous-time as a presentative model in this type.[2] The stochastic process of the conditional jump intensity is given by

$$d\lambda_u = \alpha(\theta - \lambda_u)du + \beta dJ_u, \tag{3}$$

where $\alpha > 0$, $\beta \geq 0$, and $\theta \geq 0$. In this process, past jumps raise the conditional jump intensity, and the magnitude of the effect is governed by β. It is able to generate a stronger clustering effect in jump arrivals than the affine specification (2) does. α controls the mean reversion speed of the conditional jump intensity. The unconditional jump intensity is given by $\alpha\theta/(\alpha - \beta)$.

The jump size distribution characterizes the magnitudes of jumps. The jump sizes and conditional jump intensities are assumed to be independent as in the literature. We consider the following jump size distributions. The first is the most commonly used normal distribution. The probability density function is given by

$$\nu(x) = \frac{1}{\sqrt{2\pi}} \exp\left\{ -\frac{(x - \mu_Z)^2}{2\sigma_Z^2} \right\}, \tag{4}$$

---

[2]The self-exciting jumps are considered by Aït-Sahalia, Cacho-Diaz and Laeven (2015), Fulop, Li and Yu (2015), among others. There are discrete-time autoregressive jump intensity models considered by Maheu and McCurdy (2004) and Maheu, McCurdy and Zhao (2013), which empirically capture the same effects, so we do not consider them separately here.

where μ_Z is the mean jump size and σ_Z^2 is the variance of the jump size. The second is the double exponential distribution, proposed in Kou (2002). The probability density function is given by

$$\nu(x) = \begin{cases} \frac{p}{\eta_1} \exp\{-\frac{x}{\eta_1}\} & \text{if } x \geq 0 \\ \frac{1-p}{\eta_2} \exp\{\frac{x}{\eta_2}\} & \text{if } x < 0, \end{cases} \tag{5}$$

where p is the probability of a positive jump. η_1 (η_2) measures both the mean and variance of sizes of positive (negative) jumps, with a greater value indicating a larger mean and variance. The third is the mixture of an exponential distribution and a generalized extreme value distribution. The generalized extreme value distribution is a natural candidate for the purpose of modeling jump sizes. The Fisher-Tippett theorem proves that under weak regularity conditions, the largest value in a sample drawn from an unknown distribution will converge in distribution to one of three types of probability laws, all of which belong to the generalized extreme value family. The probability density function is given by

$$\nu(x) = \begin{cases} \frac{p}{\eta} \exp\{-\frac{x}{\eta}\} & \text{if } x \geq 0 \\ \frac{1-p}{k\xi} \exp\{-(1+\frac{-x-k}{k})^{-1/\xi}\}(1+\frac{-x-k}{k})^{-1-1/\xi} & \text{if } x < 0. \end{cases} \tag{6}$$

The mixture distribution is motivated by the fact that the left tail of the return distribution is generally thicker than the right tail.[3] The distribution of the sizes of negative jumps is modeled by a restricted version of the generalized extreme value distribution, where k is the location parameter, and ξ is the shape parameter, which controls the behavior of the tail of the distribution. A higher value of ξ gives a thicker tail, and ξ is constrained to be less than 0.5 to ensure that the variance of the distribution is finite. The scale parameter in the generalized extreme value distribution is restricted to be $k\xi$ so that the support of this distribution is $(-\infty, 0)$. Figlewski (2010) uses the generalized extreme value distribution to model the tails of the risk-neutral distribution of the S&P 500 index returns.

---

[3]We also consider the case of double generalized extreme value distribution. The empirical results suggest that the double generalized extreme value distribution does not improve upon the mixture distribution because the right tail of the return distribution is not as thick as the left tail. Therefore, we do not report the results for this case.

2.2. Estimation Methodology

The discretized version of (1) is given by,

$$R_{t+1} = S_{t+1} - S_t = \mu_t + \sqrt{V_t}\varepsilon_{t+1} + \sum_{i=1}^{J_{t+1}} Z_i, \tag{7}$$

where ε_{t+1} is a standard normal random variable, J_{t+1} is the number of jumps occurred in $(t, t+1]$ with the conditional jump intensity λ_t, and Z_i for $i = 1, \cdots, J_{t+1}$ are independent and identically distributed with the probability density function $\nu(\cdot)$. Since the time-series variation of the expected return is difficult to estimate, we simply restrict the expected return to be a constant μ such that $\mu_t = \mu - \lambda_t \bar{Z} - 0.5 V_t$, where $\bar{Z}$ is the average jump size. For notational convenience, the unit of time is chosen to be consistent with the frequency of the data used.

The densities of R_{t+1} conditional on J_{t+1} and V_t can be calculated easily. Conditional on $J_{t+1} = 0$, the density is given by,

$$f(R_{t+1}|J_{t+1} = 0, V_t) = \phi(R_{t+1}; \mu_t, V_t), \tag{8}$$

where $\phi(\cdot; a, b)$ denotes the normal density with mean a and variance b. Conditional on $J_{t+1} \geq 1$, R_{t+1} is the sum of a normal random variable and J_{t+1} identically distributed jump sizes, all independent with each other. The probability density function does not always have a closed-form expression, but it can be numerically evaluated. For example, the density conditional on $J_{t+1} = 1$ is given by,

$$f(R_{t+1}|J_{t+1} = 1, V_t) = (\phi(\cdot; \mu_t, V_t) * \nu(\cdot))(R_{t+1}), \tag{9}$$

where $(\phi * \nu)$ denotes the convolution of $\phi(\cdot)$ and $\nu(\cdot)$. The density conditional on J_{t+1} for $J_{t+1} > 1$ can be evaluated with additional convolutions. Then, the density of R_{t+1} conditional on V_t is given by

$$f(R_{t+1}|V_t) = \sum_{i=0}^{\infty} f(R_{t+1}, J_{t+1} = i|V_t) = \sum_{i=0}^{\infty} f(R_{t+1}|J_{t+1} = i, V_t)\text{Pr}(J_{t+1} = i|V_t), \tag{10}$$

where

$$\Pr(J_{t+1} = i | V_t) = \frac{\exp(-\lambda_t)\lambda_t^i}{i!}, \qquad (11)$$

for $i = 0, 1, \cdots$, is the probability of $J_{t+1} = i$ conditional on V_t. Given V_t, the parameters governing the dynamics of λ_t and $\nu(\cdot)$ are estimated by maximizing the log-likelihood function $\sum_{t=1}^{T-1} \log[f(R_{t+1}|V_t)]$, where T is the number of observations. For the cases of the constant jump intensity and the affine jump intensity in (2), the maximum likelihood estimation is straight-forward since λ_t is a function of parameters and observed V_t. However, for the case of the self-exciting jump intensity in (3), jumps J_u are unobserved, which complicates the estimation. We take the filtering approach to get around the problem.[4] The discretized version of (3) is given by,

$$\lambda_{t+1} = \lambda_t + \alpha(\theta - \lambda_t) + \beta J_{t+1}. \qquad (12)$$

We use the filtered J_{t+1}, $E[J_{t+1}|V_t, R_{t+1}]$, to replace the unobserved J_{t+1} in the estimation, where

$$E[J_{t+1}|V_t, R_{t+1}] = \sum_{i=0}^{\infty} i\Pr(J_{t+1} = i | V_t, R_{t+1}) = \frac{\sum_{i=0}^{\infty} i f(R_{t+1}, J_{t+1} = i | V_t)}{f(R_{t+1}|V_t)}, \qquad (13)$$

which can be calculated based on (10). Given the parameters and an initial value of λ_t for $t = 1$, λ_t for $t \geq 2$ can be estimated by replacing J_{t+1} by $E[J_{t+1}|V_t, R_{t+1}]$ in (12). Then, the parameters and $E[J_{t+1}|V_t, R_{t+1}]$ are estimated iteratively until they converge.

2.3. Diffusive Variance Estimation

We consider a nonparametric approach to estimating the instantaneous diffusive variance, V_t, to make more robust inferences on the jump dynamics. The approach is termed the exponentially weighted moving average with truncation. Li and Zhang (2016) compare many instantaneous diffusive variance estimators proposed in the literature in terms of

---

[4]The filtering approach has been applied in Maheu and McCurdy (2004), Maheu, McCurdy and Zhao (2013), and Christoffersen, Jacobs and Ornthanalai (2012), among others, for estimation the parameters in the dynamics of asset prices.

root-mean-square errors, and find that this approach has the smallest errors. The estimator is defined as,

$$\hat{V}_t = \frac{\sum_{i=0}^{M-1} \psi^i R_{t-i}^2 1_{\{c_L \leq |R_{t-i}| \leq c_U\}}}{\sum_{i=0}^{M-1} \psi^i 1_{\{c_L \leq |R_{t-i}| \leq c_U\}}}, \tag{14}$$

where $1_{\{.\}}$ is an indicator function, M is a window-size, $\psi \in (0,1)$ is a smoothing constant, chosen such that the following log-likelihood function is maximized, $\sum_{t=M}^{T-1}(-\log \hat{V}_t - R_{t+1}^2/\hat{V}_t)1_{\{|R_{t+1}| \leq c_U\}}$, and T is the number of return observations in the sample. If ψ is not too close to one, the weights of past return observations decay quickly and the window-size M is not crucial. Experiment with data indicates that this is the case, so we simply set $M = 126$, i.e., past return observations of the recent a half year. This estimator is similar to the commonly used exponentially weighted moving average estimator of return variance. However, because of the upper truncation, c_U, it measures the diffusive component of variance, i.e., the variance due to jumps is excluded. The lower truncation, c_L, ensures that the expected diffusive variance is the same as the one without truncations. Specifically, $c_U = 5\sqrt{\text{BV}}$, where BV is the daily bipower variation of Barndorff-Nielsen and Shephard (2004, 2006) based on the entire sample. The lower truncation is set to be the value such that $E(x^2) = E(x^2|c_L^2 \leq x^2 \leq c_U^2)$, where x follows the normal distribution with mean zero and variance BV.

3. Estimation Results

We apply the methodology to the S&P 500 index returns. The index is one of the most representative indexes of the U.S. equity market, and its dynamics are examined extensively in the literature. The daily level of the S&P 500 index from January 1950 to December 2014 is downloaded from the Yahoo! Finance.

The time-series plot of the estimated annualized diffusive volatility, $\sqrt{\hat{V}_t}$, based on the expression (14) and daily return data, is shown in Figure 1, where the optimal smoothing parameter, ψ, is 0.948. There are substantial time-series variation in $\sqrt{\hat{V}_t}$. The diffusive

volatility is high around the failure of the Franklin National bank in 1974, the market crash in 1987, the Worldcom and Enron bankruptcy in 2002, the subprime debt crisis in 2008-2009, the European sovereign debt crisis in 2010, and the U.S. debt ceiling crisis in 2011. For the rest of the periods, the diffusive volatility is relatively low.

<div align="center">

Figure 1 here

</div>

The summary statistics of daily log returns with large magnitudes, R_t, are given in Table 1. The large returns are defined relative to the diffusive volatility, $\sqrt{\hat{V}_t}$. The results suggest that large negative returns are in general more frequent and of greater magnitudes than positive ones. For example, observations of $R_t < -4\sqrt{\hat{V}_t}$ account for 0.21% of the entire sample with an average of -5.038%, and those of $R_t > 4\sqrt{\hat{V}_t}$ only account for 0.099% with an average of 4.477%. These returns are very likely to be modelled as jumps because when jumps are not allowed, daily returns follow the normal distribution with mean zero and standard deviation $\sqrt{\hat{V}_t}$ approximately, and daily returns exceeding $4\sqrt{\hat{V}_t}$ or below $-4\sqrt{\hat{V}_t}$ only account for 0.003%. The most extreme negative daily return occurs during the 1987 market crash with the magnitude exceeding 20%.

<div align="center">

Table 1 here

</div>

The parameter estimates of various models are given in Table 2. There are three types of conditional jump intensity specifications, and three types of jump size distributions, totalling nine models. For the ease of interpretation, the estimates are annualized. The first is the model with the constant jump intensity and the normal jump size distribution, denoted by C-NM, where the first letter indicates the type of the conditional jump intensity and the last two letters indicate the type of the jump size distribution. The annual jump intensity is 4.78, the mean jump size is -0.0072, and the standard deviation of the jump size is 0.023. These estimates are in line with the literature. [5] The negative average

---

[5]For example, the corresponding estimates in Andersen, Benzoni and Lund (2002) are 3.45, 0 and

jump size captures the fact that large negative returns are more frequent and of greater magnitudes than large positive returns. For the model with the constant jump intensity and the double exponential jump size distribution, denoted by C-DE, the annual jump intensity is 10.17, much higher than that from the model C-NM. p is less than 0.5, which captures the fact that large negative returns are more frequent than large positive returns. However, $\eta_1 > \eta_2$ suggests that conditional on a jump, the size of a positive jump tends to be greater than that of a negative jump. The annual jump intensity implied by the model with the constant jump intensity and the mixture of exponential and generalized extreme value jump size distribution, denote by C-GE, is 11.7, the highest among the models with the constant jump intensity. Same as that implied by the model C-DE, p is less than 0.5, suggesting that negative jumps are more frequent than positive jumps. The mean of negative jumps is 1.13%, smaller than that of positive jumps of 1.66%, and the standard deviation of negative jumps is 2.58%, greater than that of positive jumps of 1.66%.

<div style="text-align:center">Table 2 here</div>

For all the models with the affine jump intensity, the conditional jump intensity is found to be positively related to the diffusive variance. One standard deviation increase in the diffusive variance leads to an increase in the annual jump intensity of 4.41, 6.83, and 8.02, for the models A-NM, A-DE, and A-EG, respectively, where A indicates the affine jump intensity. The averages of annual jump intensity implied by models A-NM, A-DE and A-EG are 6.32, 12.34 and 15.1, respectively, higher than those implied by corresponding models with the constant jump intensity. The parameters of the jump size distributions for the affine jump intensity models are comparable with those for the models with the constant jump intensity. For the models with the autoregressive jump intensity, the positive and significant estimate of β indicates the important role of past

---

0.015 for a parametric model with the same jump intensity and jump size specifications and the square-root stochastic volatility process. The corresponding estimates in Eraker, Johannes and Polson (2003) are 1.66, -0.0175 and 0.0288 for the same model.

jumps in determining the conditional jump intensity. A jump in the past increases the annual jump intensity by 126.5, 179.2, and 157.6 for the models R-NM, R-DE, and R-EG, respectively, where R indicates the autoregressive jump intensity. The estimate of α is also large, suggesting that the conditional jump intensity reverts to the unconditional mean quickly and the impacts of past jumps are short-lived. The averages of annual jump intensity are 6.97, 17.14 and 24.75 for the models R-NM, R-DE, and R-EG, respectively, even higher than the corresponding models with the affine jump intensity. To compare the two types of time-varying conditional jump intensities, we plot the estimated conditional jump intensity, $\hat{\lambda}_t$, for the models A-EG and R-EG across time in Figure 2. For the model A-EG, the behavior of $\hat{\lambda}_t$ is similar to that of $\hat{V}_t$ since $\hat{\lambda}_t$ is an affine function of $\hat{V}_t$. $\hat{\lambda}_t$ is persistent and ranges from less than 10 to below 90. For the model R-EG, $\hat{\lambda}_t$ is less persistent and moves quickly across time. The range of $\hat{\lambda}_t$ is also much wider, and the highest $\hat{\lambda}_t$ is near 340. p for both the double exponential distribution and the mixture distribution is still less than 0.5 for the models with the autoregressive jump intensity. κ and ξ for the model R-EG are notably smaller than those for the models C-EG and A-EG, which suggests that the mean, standard deviation, and thickness of the tail of each jump are smaller when jumps are allowed to be clustered strongly.

$$\boxed{\text{Figure 2 here}}$$

The last column of Table 2 reports the log-likelihood, Akaike information criterion (AIC) and Bayesian information criterion (BIC) for each model. The results of the log-likelihood indicate that for the same jump intensity specification, the mixture of the exponential and the generalize extreme value distribution fits the data best, followed by the double exponential distribution and the normal distribution. For the same jump size distribution, the autoregressive jump intensity fits the data best, followed by the affine jump intensity and the constant jump intensity. Models with more parameters usually fit the data better, however, they are not necessarily preferred because they are less parsimony and may not perform better out-of-the-sample. The models with different numbers

of parameters can be compared based on their information criteria, which penalize models with more parameters. The penalty is greater for BIC than for AIC. The results suggest that after controlling for the number of parameters, R-EG, the model with the largest number of parameters, still outperforms other models in fitting the return data.

We further examine whether the improvement of fits is from the extreme returns or from returns with smaller magnitudes. To do so, we calculate the average log-likelihood for days with extreme returns and for days with returns of smaller magnitudes. The results in Table 3 shows that in general the average value of log-likelihood is higher for the models with the autoregressive jump intensity than models with the constant jump intensity or the diffusive jump intensity. This suggests that the autoregressive jump intensity fits the return data better than the other two jump intensity specifications do regardless the magnitudes of the return. The mixture of the exponential and the generalize extreme value jump size distribution fits both the extreme negative returns and returns with smaller magnitudes better than the normal and the double exponential jump size distributions do regardless except for moderately large positive returns in a few cases. Overall, the results suggest that the model with the autoregressive jump intensity and the mixture of the exponential and the generalize extreme value jump size distribution fit both the extreme returns and returns with smaller magnitudes better than other specifications do.

Table 3 here

To highlight the differences in fitting the extreme returns among various models, in Figure 4, we plot $\bar{\lambda}\nu(Z)$ against the jump size, Z, where $\bar{\lambda} = \sum_{t=1}^{T} \hat{\lambda}_t$, is the average daily jump intensity, $\nu(Z)$ is the probability density function of the jump size. Note that the x-axis starts at -0.06 and 0.06 to highlight the density of jump sizes with large magnitudes. The figure shows the average daily intensity of jumps with various sizes. For negative jumps, the normal distribution implies more jumps of smaller magnitudes than the other two do, and the mixture of the exponential and the generalized extreme value

13

distribution has the fattest tail and implies most extreme negative jumps. The intensity of positive jumps is lower than that of negative jumps. Since the right tails from the double exponential distribution and the mixture distribution are both modeled by the exponential distribution, they behave very similarly. The normal distribution also implies a lower higher intensity for positive jumps than the other two distributions do regardless the jump sizes.

Figure 3 here

In Figure 4 and 5, we plot $\hat{\lambda}^{(10)}\nu(Z)$ and $\hat{\lambda}^{(90)}\nu(Z)$ for the models with time-varying jump intensity, where $\hat{\lambda}^{(10)}$ and $\hat{\lambda}^{(90)}$ denote the 10th and 90th percentiles of the time-series distribution of $\hat{\lambda}_t$, respectively. These two figures show the variation of the left tail and right tail due to the variation of jump intensity. The thickness of the tails implied by models with the autoregressive jump intensity varies more than that implied by models with affine jump intensities. This is the case because the autoregressive jump intensity has a greater time-series variation.

Figure 4 here

Figure 5 here

4. Jump Risk Premiums

In this section, we examine the dynamics of jump risk premiums. The jump risk premiums are inferred from the differences between the expected value of a jump measure under the risk-neutral probability, and its physical counterpart, estimated from the best specification discussed above. Intuitively, jump risk premiums are the prices that investors pay to hedge against the jump risks. We use the jump measure considered in Carr and Wu (2003) and Bollerslev and Todorov (2011). The measure under the risk-neutral probability is based

14

on the idea that short-maturity out-of-the-money options are worthless unless a jump occurs before expiration.

Specifically, the right-tail measure under the risk-neutral probability, $\tilde{\mathrm{RT}}_t(k)$, is defined as,

$$\tilde{\mathrm{RT}}_t(k) = \frac{1}{T-t}\tilde{E}_t\left(\int_t^T \tilde{\lambda}_u du\right)\int_{-\infty}^{+\infty}\max(e^x - e^k, 0)\tilde{\nu}(x)dx, \tag{15}$$

for $k > 0$, where $k = \ln(K/F_t)$, K is the strike price, and F_t is the futures price, $\tilde{\lambda}_u$ and $\tilde{\nu}(x)$ are the risk-neutral conditional jump intensity and probability density function of jump size, respectively, and $\tilde{E}_t$ denotes the expectation under the risk-neutral probability conditional on time-t information. The left-tail measure under the risk-neutral probability, $\tilde{\mathrm{LT}}_t(k)$, is defined similarly as,

$$\tilde{\mathrm{LT}}_t(k) = \frac{1}{T-t}\tilde{E}_t\left(\int_t^T \tilde{\lambda}_u du\right)\int_{-\infty}^{+\infty}\max(e^k - e^x, 0)\tilde{\nu}(x)dx, \tag{16}$$

for $k < 0$. The jump measures under the risk-neutral probability can be estimated from options prices in a model-free manner. For short-maturity options, i.e., $T \downarrow t$, it can be shown that

$$\tilde{\mathrm{RT}}_t(k) \approx \frac{e^{r_{t,T}}C_t(K)}{(T-t)F_t} \tag{17}$$

$$\tilde{\mathrm{LT}}_t(k) \approx \frac{e^{r_{t,T}}P_t(K)}{(T-t)F_t}, \tag{18}$$

where $r_{t,T}$ is the risk-free rate from t to T, and $C_t(K)$ and $P_t(K)$ are the prices of a call and a put with strike K at t, respectively.

The jump risk premiums are defined as,

$$\mathrm{RJP}_t(k) = \tilde{\mathrm{RT}}_t(k) - \mathrm{RT}_t(k) \tag{19}$$

$$\mathrm{LJP}_t(k) = \tilde{\mathrm{LT}}_t(k) - \mathrm{LT}_t(k), \tag{20}$$

where $\mathrm{RT}_t(k)$ and $\mathrm{LT}_t(k)$ are the counterparts of $\tilde{\mathrm{RT}}_t(k)$ and $\tilde{\mathrm{LT}}_t(k)$ under the physical

15

probability. They can be approximated by,

$$\mathrm{RT}_t(k) \approx \lambda_t \int_{-\infty}^{+\infty} \max(e^x - e^k, 0)\nu(x)dx \tag{21}$$

$$\mathrm{LT}_t(k) \approx \lambda_t \int_{-\infty}^{+\infty} \max(e^k - e^x, 0)\nu(x)dx, \tag{22}$$

and the approximation error decreases to zero when $T \downarrow t$.

We estimate $\tilde{\mathrm{RT}}_t(k)$ and $\tilde{\mathrm{LT}}_t(k)$ from the daily data on the S&P 500 index option prices from January 1996 to January 2013. The option data and the risk-free rate are both from the Optionmetrics. We choose the closest-to-maturity options with at least 8 calendar days to expiration, and $k = \ln 1.1$ for $\tilde{\mathrm{RT}}_t(k)$ and $k = \ln 0.9$ for $\tilde{\mathrm{LT}}_t(k)$.[6] Specifically, we calculate the Black-Scholes implied volatilities from out-of-the-money options for that maturity, and estimate the implied volatility for the strike $K = F_t e^k$ nonparametrically using the local linear regression, where the futures price F_t is inferred from the put-call parity and the at-the-money call and put prices. Then, we calculate options prices $C_t(K)$ and $P_t(K)$ from the fitted implied volatilities. Based on the estimation results for the model R-EG, which performs the best among the models we consider, we calculate the jump measures under the physical probability, $\mathrm{RT}_t(k)$ and $\mathrm{LT}_t(k)$, according to (21) and (22), where k is chosen the same as for $\tilde{\mathrm{RT}}_t(k)$ and $\tilde{\mathrm{LT}}_t(k)$.

The time-series plots of the annualized jump risk premiums, $\mathrm{RJP}_t(k)$ and $\mathrm{LJP}_t(k)$, are shown in Figure 6. Since $\tilde{\mathrm{RT}}_t(k)$ and $\tilde{\mathrm{LT}}_t(k)$ are in general greater than $\mathrm{RT}_t(k)$ and $\mathrm{LT}_t(k)$, the jump risk premiums $\mathrm{RJP}_t(k)$ and $\mathrm{LJP}_t(k)$ are positive on average. Occasionally, $\mathrm{RJP}_t(k)$ and $\mathrm{LJP}_t(k)$ become slightly negative. $\mathrm{RJP}_t(k)$ and $\mathrm{LJP}_t(k)$ usually move in the same direction. They are persistent across time. For most of the time, $\mathrm{RJP}_t(k)$ and $\mathrm{LJP}_t(k)$ are low. There are spikes from time to time, and they are particularly high during the crisis period of 2008-2009. $\mathrm{LJP}_t(k)$ is greater than $\mathrm{RJP}_t(k)$ in general, however, their differences become narrow during 2008-2009.

---

[6]Bollerslev and Todorov (2011) show that under these choices, the approximation errors in (17) and (18) are small.

16

In the following analysis, we relate the jump risk premiums to some widely used macroeconomic variables in the asset pricing literature. These variables include the monthly growth rate of the personal consumer expenditures, PCE_t, the monthly growth rate of the industrial production, IDP_t, the monthly growth rate of the consumer price index, CPI_t, all seasonally adjusted, the term spread, TSD_t, measured by the differences in the yields on 10-year treasury bonds and 3-month treasury bills, and the credit spread, CSD_t, measured by the Moody's seasoned Aaa corporate bond yield relative to the yield on 10-year treasury bonds. All the data are from the Federal Reserve Economic Data (FRED) website. We also include the annual diffusive variance, $\hat{V}_t$, and the annual jump intensity $\hat{\lambda}_t$, estimated previously, since they are considered as state variables driving the asset price dynamics in the option pricing literature.

The regression specification is given by,

$$JP_{t+1} = \beta_0 + \sum_{i=1}^{7} \beta_i X_{t,i} + \beta_8 JP_t + \varepsilon_{t+1} \tag{23}$$

where JP_t is RJP_t or LJP_t, the jump risk premium measured at the end of month t, and $X_t = (PCE_t, IDP_t, CPI_t, TSD_t, CSD_t, \hat{V}_t, \hat{\lambda}_t)$. We use the monthly data because PCE_t, IDP_t and CPI_t are available at the monthly frequency. We also control for the lagged RJP_t or LJP_t since they are persistent.

The correlations of the variables used in the regressions are shown in Table 4. RJP_{t+1} and LJP_{t+1} are negatively correlated with PCE_t, IDP_t and CPI_t, suggesting that the jump risk premiums tend to be high when the consumption, production and inflation are low, i.e., the economy is not in good conditions. RJP_{t+1} and LJP_{t+1} are positively correlated with CSD_t, $\hat{V}_t$ and $\hat{\lambda}_t$, suggesting that the jump risk premiums tend to be high in the period of high credit risk, high volatility and high jump intensity. RJP_{t+1} and LJP_{t+1} are also positively correlated with the term spread, TSD_t. RJP_{t+1} and LJP_{t+1} themselves are strongly positively correlated. Many of the macroeconomic variables are highly correlated,

in particular the pairs of $\hat{V}_t$ and CSD_t, and of CSD_t and TSD_t.

Table 4 here

The regression results are shown in Table 5. Controlling for RJP_t, PCE_t and IDP_t are still negatively related to RJP_{t+1}, and IDP_t is also significant. The coefficient on CPI_t becomes positive and insignificant. The signs on TSD_t, CSD_t, $\hat{V}_t$, and $\hat{\lambda}_t$ are still positive, and both CSD_t and $\hat{V}_t$ are significant. The lagged RJP_t is the most significant. In the multiple regressions, IDP_t and $\hat{V}_t$ are still significant, TSD_t becomes more significant, but CSD_t loses its explanatory power and the sign changes to negative. The regressions results for LJP_{t+1} reported in Panel B are similar to those for RJP_{t+1}, except that PCE_t is more significant, but IDP_t, CSD_t and $\hat{V}_t$ are only marginally significant. PCE_t is the most significant one in the multiple regression. The lagged LJP_t remains significant in specifications. Overall, the results suggest that the jump risk premiums are related to the macroeconomic conditions. The jump risk premiums tend to be high when the growths of consumption and production are low and when the credit spread and volatility are high.

Table 5 here

5. Conclusion

We investigate the dynamics of jumps in asset prices in this paper. We propose a robust approach to examining the popular specifications of the conditional jump intensity and the jump size distribution in the literature. The approach is applied to the S&P 500 index returns. The empirical results show that the model with the autoregressive jump intensity fits the data better than that with the constant jump intensity or with the jump intensity as an affine function of the diffusive variance. The autoregressive jump intensity model captures the strong clustering effects in the jump intensity process that the other specifications do not. The mixture of the exponential and generalized extreme value distribution

18

characterizes the jump size better than the commonly used normal distribution or the double exponential distribution. The generalized extreme value distribution is especially useful in modeling the fat left tail of the return distribution. We further investigate the premiums associated with the jump risks. The premiums are defined as the differences in the expected value of a jump measure under the risk-neutral probability and the physical probability. We find that jump risks carry significant premiums which are closely related to the macroeconomic conditions. In particular, the jump risk premiums are high when the growths of consumption and production in the economy are low and when the credit risk and volatility are high.

References

Aït-Sahalia, Yacine, Julio Cacho-Diaz, and Roger J. A. Laeven, 2015, Modeling financial contagion using mutually exciting jump processes, Journal of Financial Economics, 117, 585-606.

Andersen, Torben G., Luca Benzoni, and Jesper Lund, 2002, An empirical investigation of continuous-time equity return models, Journal of Finance, 57, 1239-1284.

Barndorff-Nielsen, Ole E. and Neil Shephard, 2004, Power and bipower variation with stochastic volatility and jumps, Journal of Financial Econometrics, 2, 1-37.

Barndorff-Nielsen, Ole E. and Neil Shephard, 2006, Econometrics of testing for jumps in financial economics using bipower variation, Journal of Financial Econometrics, 4, 1-30.

Bates, David S., 2000, Post-'87 crash fears in the S&P 500 futures option market, Journal of Econometrics, 94, 181-238.

Bollerslev, Tim and Viktor Todorov, 2011, Tails, fears, and risk premia, Journal of Finance, 66, 2165-2211.

1829-1857.

Carr, Peter and Liuren Wu, 2003, What type of process underlies options? A simple robust test, Journal of Finance, 58, 2581-2610.

Chan, Wing H. and John M. Maheu, 2002, Conditional jump dynamics in stock market returns, Journal of Business and Economic Statistics, 20, 377-389.

Christoffersen, Peter, Kris Jacobs, and Karim Mimouni, 2010, Volatility dynamics for the S&P 500: Evidence from realized volatility, daily returns, and option prices, Review of Financial Studies, 23, 3141-3189.

Christoffersen, Peter, Kris Jacobs, and Chayawat Ornthanalai, 2012, Dynamic jump intensities and risk premiums: Evidence from S&P500 returns and options, Journal of Financial Economics, 106, 447-472.

Duffie, Darrell, Jun Pan, and Kenneth Singleton, 2000, Transform analysis and asset pricing for affine jump-diffusions, Econometrica, 68, 1343-1376.

Eraker, Bjorn, 2004, Do stock prices and volatility jump? Reconciling evidence from spot and option prices, Journal of Finance, 59, 1367-1403.

Eraker, Bjorn, Michael Johannes, and Nicholas Polson, 2003, The impact of jumps in volatility and returns, Journal of Finance, 58, 1269-1300.

Figlewski, Stephen, 2010, Estimating the implied risk neutral density for the U.S. market portfolio, In: Tim Bollerslev, Jeffrey R. Russell and Mark Watson (Ed.), Volatility and time series econometrics: Essays in honor of Robert F. Engle, Oxford University Press, Oxford, UK, pp. 323-353.

Fulop, Andras, Junye Li, and Jun Yu, 2015, Self-exciting jumps, learning, and asset pricing implications, Review of Financial Studies, 28, 876-912.

Heston, Steven L, 1993, A closed-form solution for options with stochastic volatility, with applications to bond and currency options, Review of Financial Studies, 6, 327-343.

Jones, Christopher S., 2003, The dynamics of stochastic volatility: Evidence from underlying and option markets, Journal of Econometrics, 116, 181-224.

Kou, S.G., 2002, A jump-diffusion model for option pricing, Management Science, 48, 1086-1101.

Li, Gang and Chu Zhang, 2013, Diagnosing affine models of options pricing: Evidence from VIX, Journal of Financial Economics, 107, 199-219.

Li, Gang and Chu Zhang, 2016, On the relationship between conditional jump intensity and diffusive volatility, Journal of Empirical Finance, 37, 196-213.

Maheu, John M. and Thomas H. McCurdy, 2004, News arrival, jump dynamics and volatility components for individual stock returns, Journal of Finance, 59, 755793.

Maheu, John M., Thomas H. McCurdy, and Xiaofei Zhao, 2013, Do jumps contribute to the dynamics of the equity premium? Journal of Financial Economics, 110, 457-477.

Merton, Robert C., 1976, Option pricing when underlying stock returns are discontinuous, Journal of Financial Economics, 3, 125-144.

Newey, Whitney K. and Kenneth D. West, 1987, A simple, positive semi-definite, heteroscedasticity and autocorrelation consistent covariance matrix, Econometrica, 55, 703-708.

Pan, Jun, 2002, The jump-risk premia implicit in options: Evidence from an integrated time-series study, Journal of Financial Economics, 63, 3-50.

Santa-Clara, Pedro and Shu Yan, 2010, Crashes, volatility, and the equity premium: Lessons from S&P 500 options, Review of Economics and Statistics, 92, 435-451.

Yu, Jun, 2004, Empirical characteristic function estimation and its applications, Econometric Reviews, 23, 93-123.

Table 1
Summary Statistics of Large Returns

This table reports the frequency (freq), mean, standard deviation (std), skewness (skew) and kurtosis (kurt) of daily log returns with large magnitudes, R_t, of the S&P 500 index from July 1950 to December 2014. The large returns are defined relative to the diffusive volatility, $\sqrt{\hat{V}_t}$.

R_{t+1}	$> 2\sqrt{\hat{V}_t}$	$> 3\sqrt{\hat{V}_t}$	$> 4\sqrt{\hat{V}_t}$	$> 5\sqrt{\hat{V}_t}$	$< -2\sqrt{\hat{V}_t}$	$< -3\sqrt{\hat{V}_t}$	$< -4\sqrt{\hat{V}_t}$	$< -5\sqrt{\hat{V}_t}$
freq(%)	2.742	0.382	0.099	0.031	3.340	0.684	0.210	0.080
mean(%)	2.200	3.352	4.477	6.223	-2.190	-3.267	-5.038	-6.590
std(%)	1.248	1.912	2.244	3.428	1.581	2.711	3.921	5.313
skew	2.566	2.180	1.983	0.504	-5.530	-3.966	-2.875	-2.370
kurt	13.873	8.408	5.935	1.524	59.642	26.448	13.687	8.123

Table 2
Parameter Estimates

This table reports parameter estimates of the asset price processes and their standard errors in parentheses. The last column reports the value of log-likelihood function (LL), Akaike information criterion (AIC) and Bayesian information criterion (BIC). C-NM, C-DE and C-EG are the models with the constant jump intensity and the normal, double exponential and mixture of exponential and generalized extreme value jump size distribution, respectively. A-NM, A-DE and A-EG are the models with the affine jump intensity and these jump size distributions, and R-NM, R-DE and R-EG are the models with the autoregressive jump intensity. The parameters for the jump intensity and μ are annualized.

model	jump intensity				jump size				model fit	
C-NM	μ	λ			μ_Z	σ_Z			LL	55435
	0.0586	4.783			-0.0072	0.0229			AIC	-110862
	(0.015)	(0.77)			(0.002)	(0.003)			BIC	-110831
C-DE	μ	λ			p	η_1	η_2		LL	55465
	0.0583	10.167			0.1119	0.0180	0.0107		AIC	-110920
	(0.015)	(1.65)			(0.043)	(0.004)	(0.001)		BIC	-110881
C-EG	μ	λ			p	η	κ	ξ	LL	55489
	0.0613	11.702			0.1106	0.0166	0.0075	0.4068	AIC	-110965
	(0.015)	(1.82)			(0.041)	(0.004)	(0.001)	(0.030)	BIC	-110919
A-NM	μ	λ_0	λ_1		μ_Z	σ_Z			LL	55449
	0.0622	1.855	219.07		-0.0068	0.0226			AIC	-110887
	(0.014)	(0.76)	(57.3)		(0.002)	(0.002)			BIC	-110849
A-DE	μ	λ_0	λ_1		p	η_1	η_2		LL	55475
	0.0616	5.437	339.23		0.1544	0.0151	0.0111		AIC	-110937
	(0.015)	(1.56)	(98.5)		(0.056)	(0.003)	(0.001)		BIC	-110891
A-EG	μ	λ_0	λ_1		p	η	κ	ξ	LL	55498
	0.0638	7.002	397.92		0.1145	0.0156	0.0076	0.4005	AIC	-110982
	(0.015)	(1.75)	(121)		(0.043)	(0.003)	(0.001)	(0.027)	BIC	-110929
R-NM	μ	α	β	θ	μ_Z	σ_Z			LL	55503
	0.0667	191.41	126.52	2.3615	-0.0049	0.0218			AIC	-110995
	(0.014)	(31.5)	(31.3)	(0.619)	(0.001)	(0.002)			BIC	-110948
R-DE	μ	α	β	θ	p	η_1	η_2		LL	55544
	0.0724	222.43	179.22	3.3296	0.2086	0.0131	0.0100		AIC	-111074
	(0.015)	(31.8)	(38.0)	(1.159)	(0.070)	(0.003)	(0.001)		BIC	-111021
R-EG	μ	α	β	θ	p	η	κ	ξ	LL	55590
	0.0794	188.80	157.56	4.0952	0.1311	0.0142	0.0069	0.3549	AIC	-111163
	(0.015)	(25.6)	(28.9)	(1.221)	(0.047)	(0.003)	(0.000)	(0.020)	BIC	-111102

Table 3
Model Performance

This table reports the average value of log-likelihood function, $\log[f(R_{t+1}|V_t)]$, for days with returns of various magnitudes. The ranges of returns are given in the first column. C-NM, C-DE and C-EG are the models with the constant jump intensity and the normal, double exponential and mixture of exponential and generalized extreme value jump size distribution, respectively. A-NM, A-DE and A-EG are the models with the affine jump intensity and these jump size distributions, and R-NM, R-DE and R-EG are the models with the autoregressive jump intensity.

R_{t+1}	C-NM	C-DE	C-EG	A-NM	A-DE	A-EG	R-NM	R-DE	R-EG
$\in [-0.06, 0.06]$	3.428	3.429	3.430	3.428	3.429	3.430	3.430	3.433	3.436
> 0.06	-3.097	-2.710	-2.750	-2.482	-2.296	-2.281	-1.789	-1.850	-1.851
> 0.075	-6.859	-5.825	-5.936	-5.634	-5.035	-5.006	-3.696	-3.829	-3.857
> 0.1	-6.587	-5.782	-5.877	-5.241	-4.821	-4.797	-4.231	-4.178	-4.126
< -0.06	-4.779	-4.734	-4.199	-4.067	-4.030	-3.623	-3.792	-3.851	-3.640
< -0.075	-7.963	-7.224	-5.508	-6.672	-6.005	-4.525	-5.827	-5.644	-4.436
< -0.1	-24.828	-19.137	-9.234	-23.537	-17.594	-8.523	-21.522	-16.846	-7.897

Table 4
Correlations among Jump Risk Premiums and Macroeconomic Variables
This table reports the correlations among the following variables: the jump risk premiums on the right tail and the left tail, RJP_{t+1} and LJP_{t+1}, the monthly growth rate of the personal consumer expenditures, PCE_t, the monthly growth rate of the industrial production, IDP_t, the monthly growth rate of the consumer price index, CPI_t, all seasonally adjusted, the term spread, TSD_t, measured by the differences in the yields on 10-year treasury bonds and 3-month treasury bills, the credit spread, CSD_t, measured by the Moody's seasoned Aaa corporate bond yield relative to the yield on 10-year treasury bonds, the diffusive variance, $\hat{V}_t$, and the jump intensity, $\hat{\lambda}_t$. All the variables are measured at the end of month t.

	RJP_{t+1}	LJP_{t+1}	PCE_t	IDP_t	CPI_t	TSD_t	CSD_t	$\hat{V}_t$
LJP_{t+1}	0.926							
PCE_t	-0.344	-0.355						
IDP_t	-0.429	-0.358	0.270					
CPI_t	-0.260	-0.270	0.376	0.049				
TSD_t	0.200	0.197	-0.143	-0.054	-0.100			
CSD_t	0.434	0.468	-0.267	-0.355	-0.210	0.485		
$\hat{V}_t$	0.646	0.671	-0.356	-0.339	-0.326	0.207	0.680	
$\hat{\lambda}_t$	0.394	0.444	-0.151	-0.094	-0.074	0.004	0.119	0.281

Table 5
Jump Risk Premiums and Macroeconomic Variables

This table reports the coefficient estimates of the following regression,

$$\text{JP}_{t+1} = \beta_0 + \sum_{i=1}^{7} \beta_i X_{t,i} + \beta_8 \text{JP}_t + \varepsilon_{t+1}$$

where JP_t is RJP_t or LJP_t, the jump risk premium on the right tail or the left tail, $X_t = (\text{PCE}_t, \text{IDP}_t, \text{CPI}_t, \text{TSD}_t, \text{CSD}_t, \hat{V}_t, \hat{\lambda}_t)$, PCE_t is the monthly growth rate of the personal consumer expenditures, IDP_t is the monthly growth rate of the industrial production, CPI_t is the monthly growth rate of the consumer price index, TSD_t is the term spread, CSD_t is the credit spread, $\hat{V}_t$ is the annual diffusive variance, and $\hat{\lambda}_t$ is the annual jump intensity. The data are measured at the end of month t. The heteroscedasticity and serial correlation consistent t-statistics based on the Newey and West (1987) procedure with 3 lags are reported in the parentheses.

A. RJP_{t+1}

Const	PCE_t	IDP_t	CPI_t	TSD_t	CSD_t	$\hat{V}_t$	$\hat{\lambda}_t$	RJP_t	R^2
0.006	-0.522							0.658	0.486
(2.56)	(-1.40)							(7.22)	
0.006		-1.008						0.622	0.545
(3.54)		(-2.57)						(6.44)	
0.003			0.311					0.706	0.480
(1.91)			(0.56)					(6.65)	
0.001				0.138				0.680	0.483
(1.07)				(1.69)				(6.85)	
-0.005					0.623			0.635	0.489
(-1.63)					(2.24)			(5.84)	
-0.003						0.260		0.480	0.509
(-1.53)						(2.50)		(3.87)	
0.000							0.041	0.632	0.507
(0.09)							(1.16)	(7.62)	
0.001	-0.136	-0.940	0.093	0.212	-0.492	0.221	0.040	0.408	0.592
(0.20)	(-0.59)	(-2.96)	(0.15)	(2.15)	(-1.67)	(2.28)	(1.63)	(4.01)	

B. LJP_{t+1}

| Const	PCE_t	IDP_t	CPI_t	TSD_t	CSD_t	$\hat{V}_t$	$\hat{\lambda}_t$	LJP_t	R^2
0.016	-1.291							0.708	0.572
(4.30)	(-2.31)							(13.03)	
0.013		-1.363						0.703	0.598
(4.40)		(-1.73)						(12.92)	
0.008			0.505					0.760	0.560
(2.79)			(0.62)					(11.20)	
0.007				0.191				0.738	0.562
(2.36)				(1.30)				(11.88)	
0.000					0.769			0.705	0.564
(-0.08)					(1.68)			(10.21)	
0.005						0.269		0.616	0.567
(1.90)						(1.75)		(6.52)	
0.006							0.056	0.687	0.575
(1.59)							(0.89)	(11.68)	
0.010	-0.826	-1.180	0.464	0.243	-0.295	0.185	0.061	0.542	0.625
(1.17)	(-2.11)	(-1.70)	(0.49)	(1.34)	(-0.58)	(1.08)	(1.29)	(5.32)	
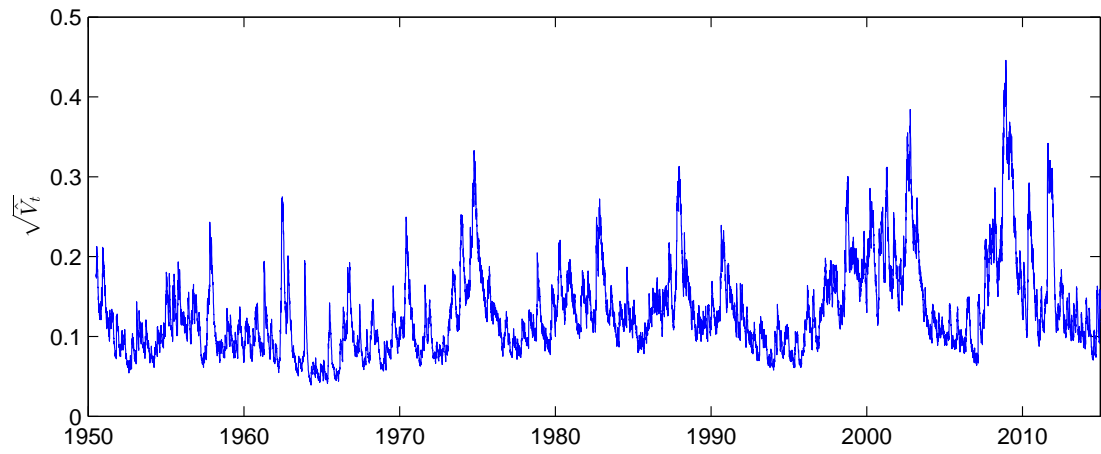
Figure 1. Diffusive Volatility

This figure shows the time-series plot of the estiamted annualized diffusive volatility, $\sqrt{\hat{V}_t}$.
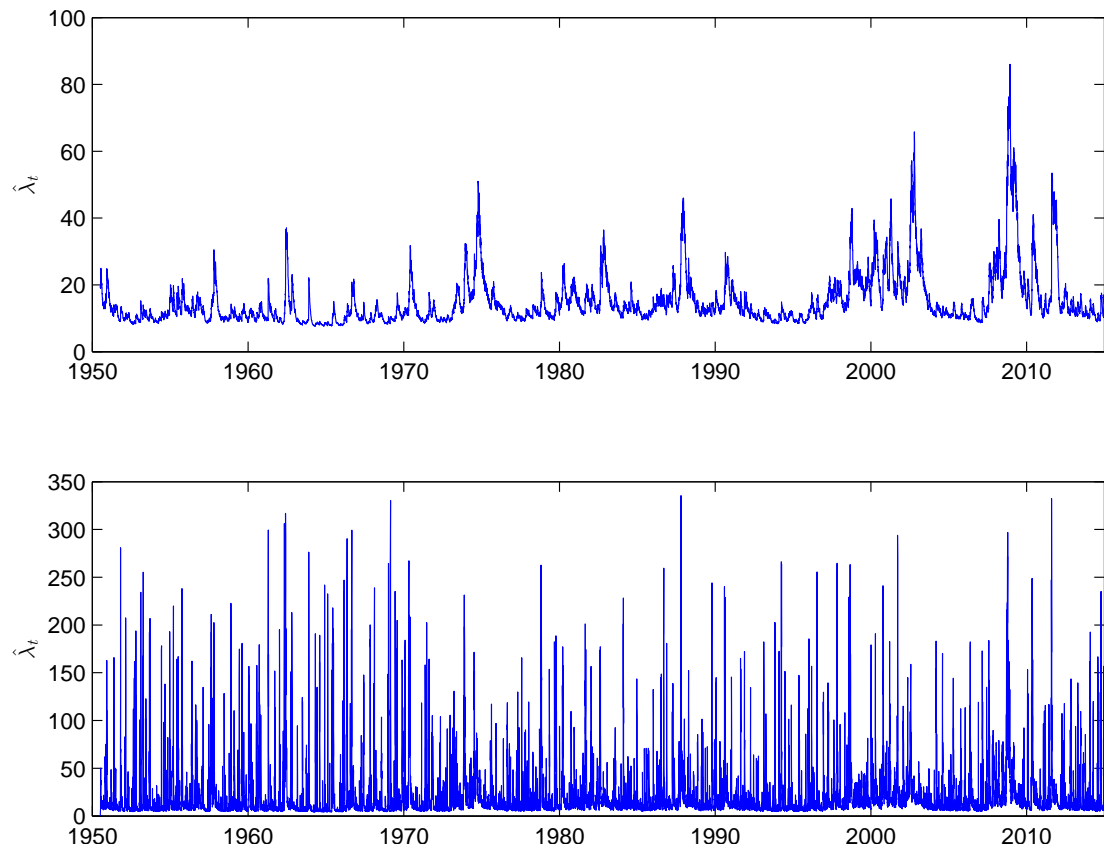
Figure 2. Conditional Jump Intensity

This figure shows the time-series plots of the estimated annual conditional jump intensity, $\hat{\lambda}_t$. The upper panel is from the model A-EG, the affine jump intensity and the mixture of exponential and generalized extreme value jump size distribution, and the lower panel is from the model R-EG, the autoregressive jump intensity and the mixture of exponential and generalized extreme value jump size distribution.
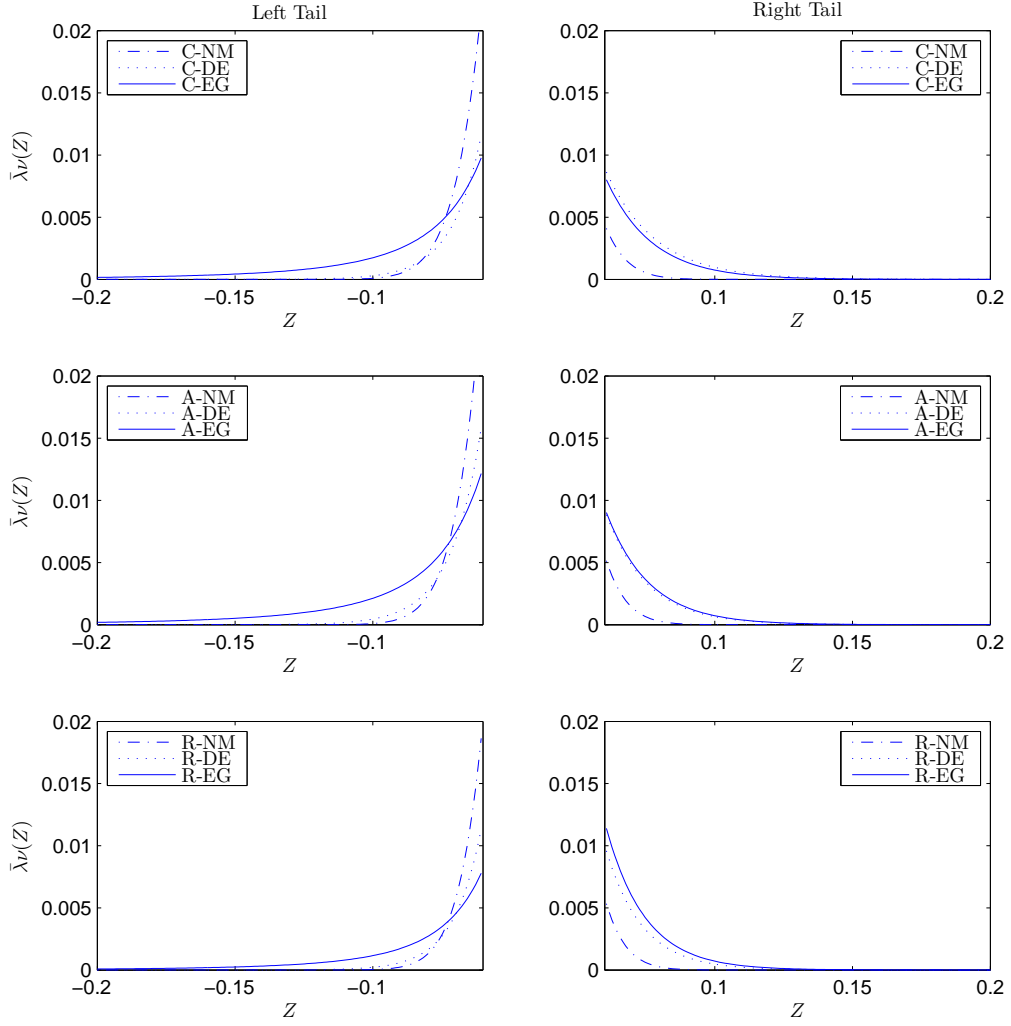
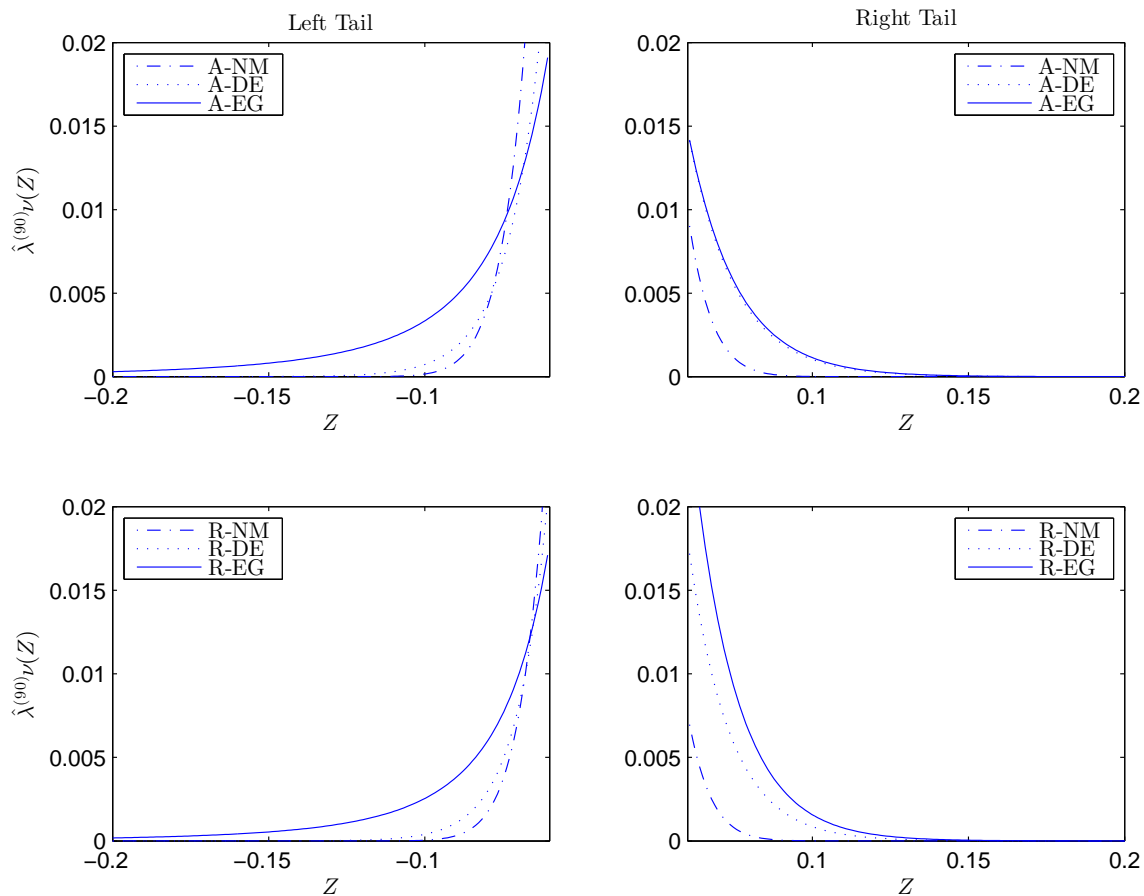**Figure 3. Jump Size Distribution (at the average jump intensity)**

This figure plots $\bar{\lambda}\nu(Z)$ as a function of Z, where Z is the jump size, $\bar{\lambda} = \sum_{t=1}^{T} \hat{\lambda}_t$, is the average daily jump intensity, and $\nu(Z)$ is the probability density function of Z. The left panels show the left tails of the densities, and the right panels show the right tails of the densities. C-NM, C-DE and C-EG are the models with the constant jump intensity and the normal, double exponential and mixture of exponential and generalized extreme value jump size distribution, respectively. A-NM, A-DE and A-EG are the models of the affine jump intensity and these jump size distributions, and R-NM, R-DE and R-EG are the models of the autoregressive jump intensity.
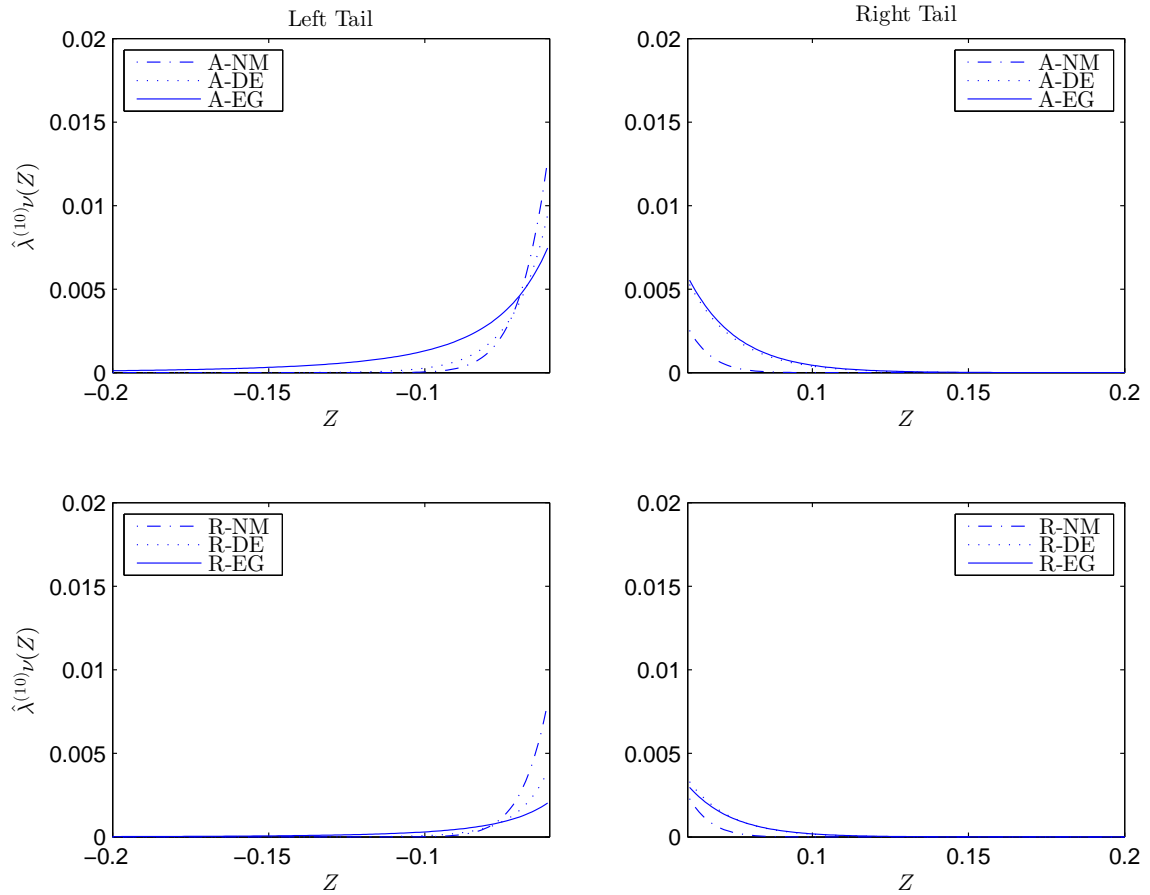
Figure 4. Jump Size Distribution (at the 10th percentile of the jump intensity)
This figure plots $\hat{\lambda}^{(10)}\nu(Z)$ as a function of Z, where Z is the jump size, $\hat{\lambda}^{(10)}$ is the 10th percentile of the distribution of the daily jump intensity, and $\nu(Z)$ is the probability density function of Z. The left panels show the left tails of the densities, and the right panels show the right tails of the densities. A-NM, A-DE and A-EG are the models of the affine jump intensity and the normal, double exponential and mixture of exponential and generalized extreme value jump size distribution, respectively, and R-NM, R-DE and R-EG are the models of the autoregressive jump intensity and these jump size distributions.

Figure 5. Jump Size Distribution (at the 90th percentile of the jump intensity)
This figure plots $\hat{\lambda}^{(90)}\nu(Z)$ as a function of Z, where Z is the jump size, $\hat{\lambda}^{(90)}$ is the 90th percentile of the distribution of the daily jump intensity, and $\nu(Z)$ is the probability density function of Z. The left panels show the left tails of the densities, and the right panels show the right tails of the densities. A-NM, A-DE and A-EG are the models of the affine jump intensity and the normal, double exponential and mixture of exponential and generalized extreme value jump size distribution, respectively, and R-NM, R-DE and R-EG are the models of the autoregressive jump intensity and these jump size distributions.
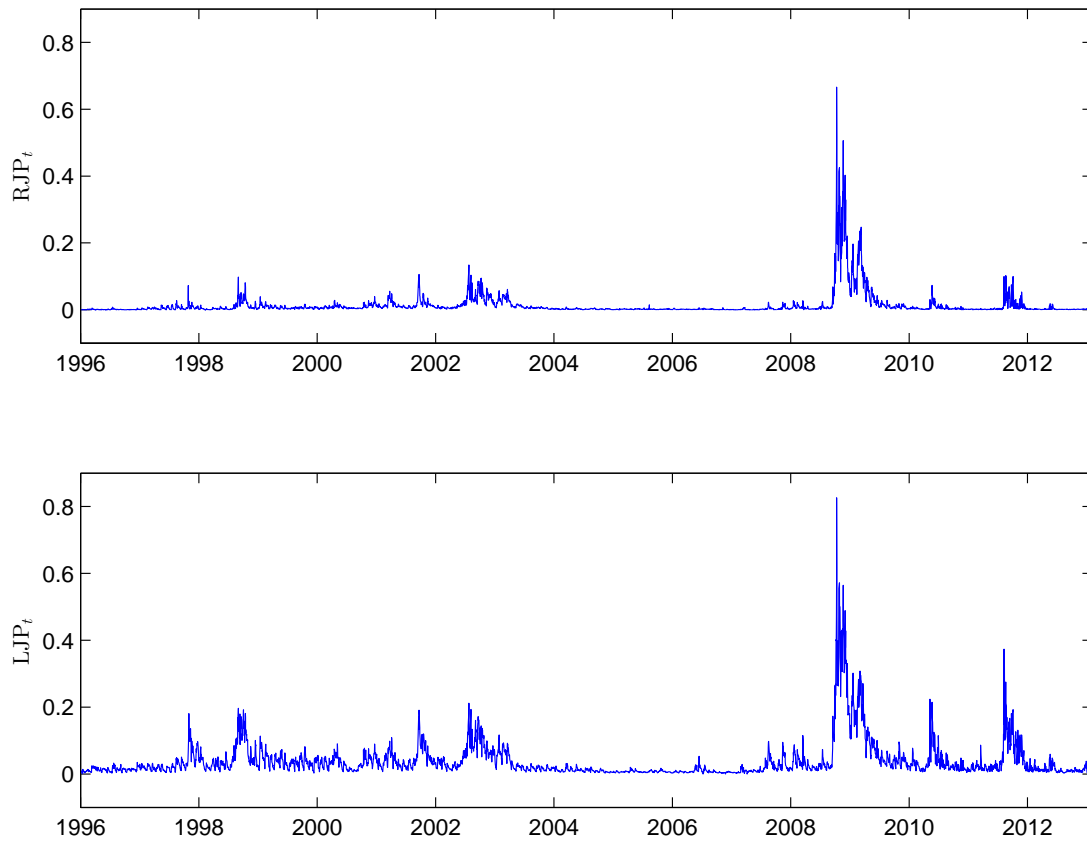
Figure 6. Jump Risk Premiums

This figure shows the time-series plots of the annual jump risk premiums. The upper panel is the jump risk premium from the right tail of the return distribution, RJP_t, and the lower panel is the jump risk premium from the left tail of the return distribution, LJP_t.